EUMETSAT Satellite Application Facility on
Support to Operational Hydrology and Water Management

Algorithm Theoretical Baseline Document (ATBD) for product P-IN-FCI (H40)

Precipitation rate at ground by MTG FCI IR channel supported by LEO/MW

Reference Number:	SAF/HSAF/ATBD-40
Issue/Revision Index:	1.1
Last Change:	14/11/2019

DOCUMENT CHANGE RECORD

Issue / Revision	Date	Description
0.1	02/03/2015	Version prepared for PDR
0.2	31/10/2017	MTG-PDR RIDs implemented
1.0	01/06/2018	Version prepared for MTG CDR
1.1	14/11/2019	Version prepared for MTG SIRR

INDEX

1 Introduction to P-IN-FCI (H40)

IN P-IN-FCI product, instantaneous precipitation map is generated by IR images from MTG- FCI (MTG FCI L1 Product User Guide) "calibrated" by precipitation estimates from MW radiometers on board of LEO satellites, processed soon after each acquisition of a new image from MTG-FCI. The calibration procedure will be carried out after each PMW radiometer overpass .

1.1 Product Heritage

Product P-IN-FCI uses the approach developed for P-IN-SEVIRI-PMW (H60) (Precipitation rate at ground by GEO/IR channel supported by LEO/MW) exploiting new capabilities of MTG FCI P-IN-SEVIRI-PMW was based on the IR images from the SEVIRI instrument on-board Meteosat Second Generation (MSG) satellites; precipitation estimates were obtained by combining SEVIRI IR GEO, equivalent blackbody temperatures (TB) at 10.8 μm, with rain rates from PMW precipitation rate estimates (P-IN-SSMIS and P-IN- MHS). The algorithm is based on a collection of overlapping (in time and space) GEO IR pixels and Low Earth Orbit (LEO) PMW sensors pixels from all available overpasses. The co-located pixels are used to build a look up table of geolocated relationships PMW rain rate vs IR TB, updated as soon as new overlapping GEO IR images and LEO PMW overpasses are available. The processing method is called "Rapid Update" (RU).In addiction P-IN_SEVIRI_PMW production chain identificates convective areas and computes a different RR-TB relationships by distinguish between convective and stratiform fields. The convective areas are identified with the automatic tool for nowcasting applications NEFODINA (Melfi et al., 2012).

1.2 MTG Programme

To understand the changes made to the P-IN_SEVIRI-PMW algorithms, for the new product, we introduce some information about the sensors which will be on board of MTG satellites.

The MTG program provides meteorological imagery over Europe and Africa and maintains continuity of the Meteosat program, continuing and expanding the service provide by MSG. The MTG system will be operated by EUMETSAT and will provide Europe's national meteorological services as well as international users and science community with improved imaging and new infrared sounding capabilities for both meteorological and climate applications. The MTG program is established as a common undertaking between EUMETSAT and the European Space Agency (ESA). ESA is responsible for the development of the MTG space segment. EUMETSAT is responsible for the development of the MTG ground segment and service provision. Thanks to advances in technology, MTG will also provide an enhanced service compared to the current MSG system, contributing significant improvements to the existing service with an improved imagery mission (Flexible Combined Imager - FCI) and introducing new sounding and lightning missions (Lightning Imager - LI) from a geostationary orbit.1.2.2 The Flexible Combined Imager (FCI)
The FCI will provide follow-on services to the Full Disc Scanning Service (FDSS) and Rapid Scanning Service (RSS) currently provided by the Meteosat Second Generation (MSG) Spinning Enhanced Visible and Infrared Imager (SEVIRI). The FCI has channels over 16 spectral ranges covering visible to infrared wavelengths.

Characteristics	MSG	MTG
Full-Disk Image Cycle	15 min	10 min
Spectral Channels (μm)	VIS 0.6 VIS 0.8 NIR 1.6 IR 3.8 IR 6.2 IR 7.3 IR 8.7 IR 9.7 IR 10.8 IR 12.0 IR 13.4	**VIS 0.4** **VIS 0.5** VIS 0.6 VIS 0.8 **VIS 0.9** **NIR 1.3** NIR 1.6 **NIR 2.2** IR 3.8 **IR 6.3** IR 7.3 IR 8.7 IR 9.7 **IR 10.5** **IR 12.3** **IR 13.3**
Sampling Distance (nadir)	1Km (HRV) 3Km (others)	0.5-1 Km (VIS-NIR) 1-2 Km (IR)
Telescope Diameter	500 mm	300 mm

Table 1. Comparison between the characteristics of FCI and SEVIRI radiometers.

Table 2 shows the comparison of some technical details of the FCI and SEVIRI radiometers in order to highlight the common features and some of the enhancements of the FCI that need to be considered in the development of the P-IN-FCI product. In detail, three points need to be considered:

1. The 10.5 μm FCI channel is used in placed of the 10.8 μm SEVIRI channel.
2. The calibration procedure between MW and IR signals performed taking into account the higher resolution of the FCI radiometer.
3. The higher FCI generation frequency (10 min vs. 15 min of SEVIRI) allowing greater accuracy in the observation of a meteorological scene consistently with the current effort to reduce the temporal gap between MW satellite based rain rate estimates.

1.3 1.3 P-IN-FCI Requirements

For detailed requirements' characteristics see Product Requirement Document.

2 Processing concept

P-IN-FCI product will be based on the use of five (or more if available) MW derived products as P-IN-SEVIRI-PMW (while the P-IN-SEVIRI product was based only on two MW-derived precipitation estimates from P-IN-SSMI new release and P-IN-MHS):

MW derived products	Approach adopted	Satellites	Additional outputs
P-IN-SSMISnew release	Bayesian algorithm	SSMIS on DMSP	Quality and phase Flag provided
P-IN-MHS	Neural Network Algorithm	AMSUA-MHS on Metop and NOAA	Quality and Phase Flag provided
H-AUX-17	Bayesian algorithm	AMSR-2 on GCOM-W1	Quality and Phase Flag provided
P-IN-ATMS	Neural Network Algorithm	ATMS on SuomiNPP, JPSS	Quality and Phase Flag provided
H-AUX-20	Bayesian algorithm/ Neural Network Algorithm	GMI on GPM Core Observatory Satellite	Quality and Phase Flag provided

Table 2. Specifications of MW derived products.

For the aim of ingesting FCI data into the processing chain of the blended algorithm it is necessary to extract from the available image files the information needed. Very briefly, the essential data needed to process FCI image data are:

- the starting and ending date and time of acquisition (UTC) for each image data or area subset;
- the latitude and longitude coordinates for the geo-location of each pixel in the area;
- the Channel 14 (10.5 μm) equivalent blackbody temperature (K) for each pixel. The digital counts are converted into radiances by means of the calibration coefficients distributed along with each image data. Then, radiances are converted into equivalent blackbody temperature (TBB) by means of regression relationships and the corresponding coefficients;
- the satellite zenith angle of observation for each pixel (deg);
- the acquisition time of each pixel (or line of pixels) measured in seconds from the starting time of acquisition;
- nominal line and column number for each pixel.

3 Algorithms description

The following sections describe the principal characteristics of the various software modules that compose P-AC-FCI generation chain.

3.1 The "Rapid-Update" and NEFODINA processing chain

The adopted blended technique (Turk et al. 2000 a and b), called RU, is the same of P-IN-SEVIRI-PMW, modified with the introduction of NEFODINA algorithm and adapted to MTG-FCI data.

NEFODINA software allows to process rainy pixel of PMW radiometer orbital grid differently depending on whether rainfall is convective or stratiform. The choice of one or the other case depends on the convection file obtained by combining the information deriving from both the NEFODINA SW output (and the SEVIRI-MSG file containing the Channel 14 (10.5 μm) TB (K). When a PMW radiometer's file is selected, a cycle is performed on the number of pixels, searching the coincidence between TB from IR radiometer
and rainfall estimates from PMW radiometer based on both the geographical coordinates and time.

When the coincidence has been found, firstly, the number of pixels of MTG-FCI belonging to the selected PMW radiometer's one is identified. So, if more than one pixel of the FCI grid has been found, those referring to convective rain are counted (according to the NEFODINA software).
In that case, a factor f is calculated depending on both the overall area of the convective pixels and their number in the following way:

$$f = \frac{N^2}{A}$$

where N is the number of SEVIRI-MSG pixels and A is overall convective area in the PMR radiometer one. Then, f is utilized to correct the PMW radiometer's rainfall estimates, being the latter multiplied by the factor. However, PMW radiometer's estimates are corrected for convective case only if f is greater or equal than 1.
If any TB estimation from MTG-FCI related to the convective case belongs to the considered PMW radiometer's pixel, rainfall estimates from PMW radiometer will be not corrected, and the rain is intended to be stratiform.
Key to the RU blended satellite technique is a real time, underlying collection of time and space overlapping pixels from operational geostationary IR imagers and LEO MW sensors. Rain intensity maps derived from MW measurements are used to create geo-located rain rate (RR) vs TB relationships, that are renewed as soon as new co-located data are available from both geostationary and MW instruments. In the software package these relationships are called histograms. To the end of geo-locating histogram relationships, the study area is subdivided in equally spaced lat-lon boxes (2.5° x 2.5°).

As new input datasets (MW and IR) are available in the processing chain, the MW-derived RR pixels are paired with their time and space-coincident geostationary 10.5-μm IR TB data, using a 10-minute maximum allowed time offset between the pixel acquisition times and a maximum space offset of 10 km between the pixel coordinates. Each co-located data increments histograms of TB and RR in the nearest 2.5° latitude-longitude box, as well in the eight surrounding boxes (this overlap ensures a fairly smooth transition in the histogram shape between neighboring boxes). The rational behind these threshold values for time collocation and box size is discussed by Turk et al. 2002.

In order to set-up a meaningful statistical ensemble, the method can look at older MW-IR slot intersections (no older than 24 h), until a certain (75 %) box coverage is reached and a minimum number of coincident observations are gathered for a 2.5° x 2.5° region (at present 400 points, this is a tunable parameter in the procedure). Thus RU requires an initial start-up time period (~ 24 h), to allow for establishing meaningful, initial relationships all over the study area.
As soon as a box is refreshed with new data, a probabilistic histogram matching relationship (Calheiros and Zawadzki, 1987) is updated using the MW RR and IR TB probability distribution functions (PDF), and an updated lookup table (histogram file) is created. The matching is performed as follows:

$$\int_{R_T}^{R_i} p(R)dR = \int_{TBB(T)}^{TBB(i)} p(T_{BB})dT_{BB},$$

where p(R) and p(TB) are the PDF of RR and TB respectively, and RT and TB(T) are the threshold values.
Examples of TB vs RR relationships (histogram) are presented in Fig. 1.

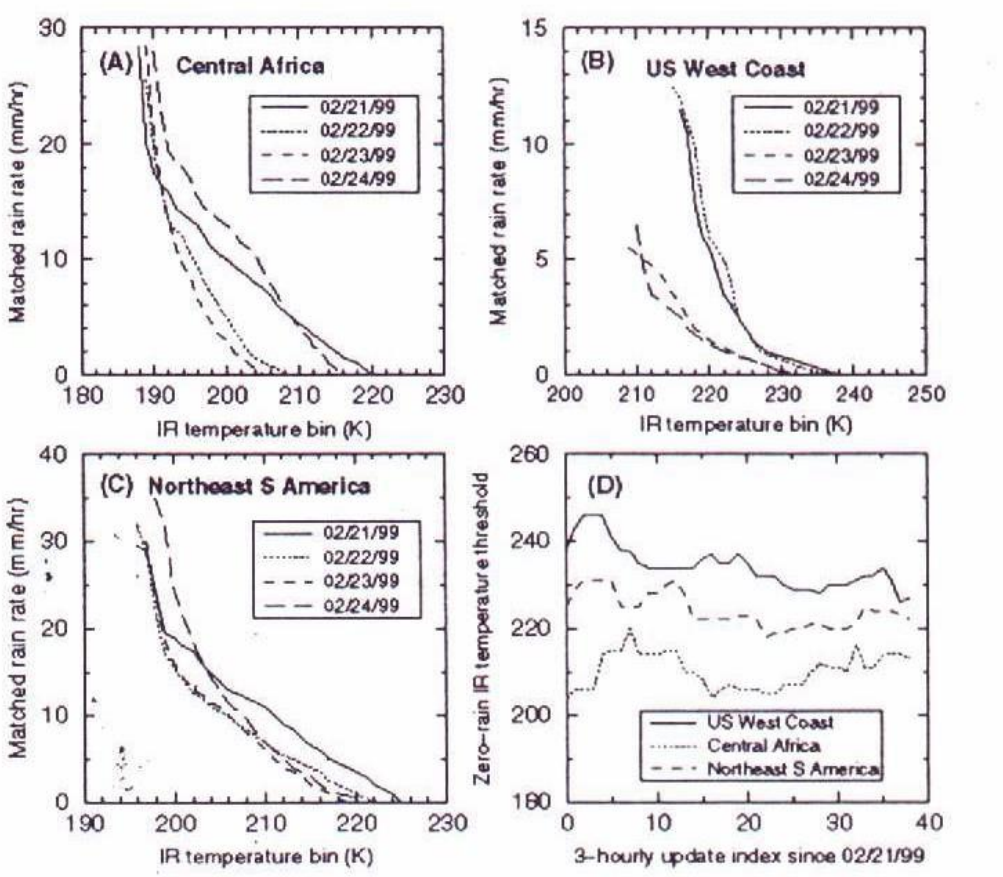

Figure 1. Rain rate vs brightness temperature average relationships for the days and geographical areas marked. (D) presents the zero-rain thresholds as a function of time.

The global histograms update process is constantly on-going along with the operational input of MW and geostationary datasets. The transfer of this "background" information to the stream of steadily arriving GEO data involves a computationally fast lookup table and interpolation process for each pixel in the geostationary datasets. For each FCI pixel the RR is finally computed by interpolating the proper TB vs RR histogram, firstly smoothed using the relationships of the surrounding boxes in order to ensure a smooth transition in RR across box boundaries.

If any histogram is more than 24-hours old relative to the IR dataset time, that histogram is not used. In this case a conventional rain rate value = -1 is assigned to each pixel. However, in ordinary operations, the case is only theoretical since, considering the suite of MW data in input to the algorithm, a histogram more recent than 24 hours is nearly always available. In case of a prolonged interruption of the input data stream (either MW or IR data) the blended product cannot be produced and delivered. Moreover, it will require a start-up period of several hours to restart properly.

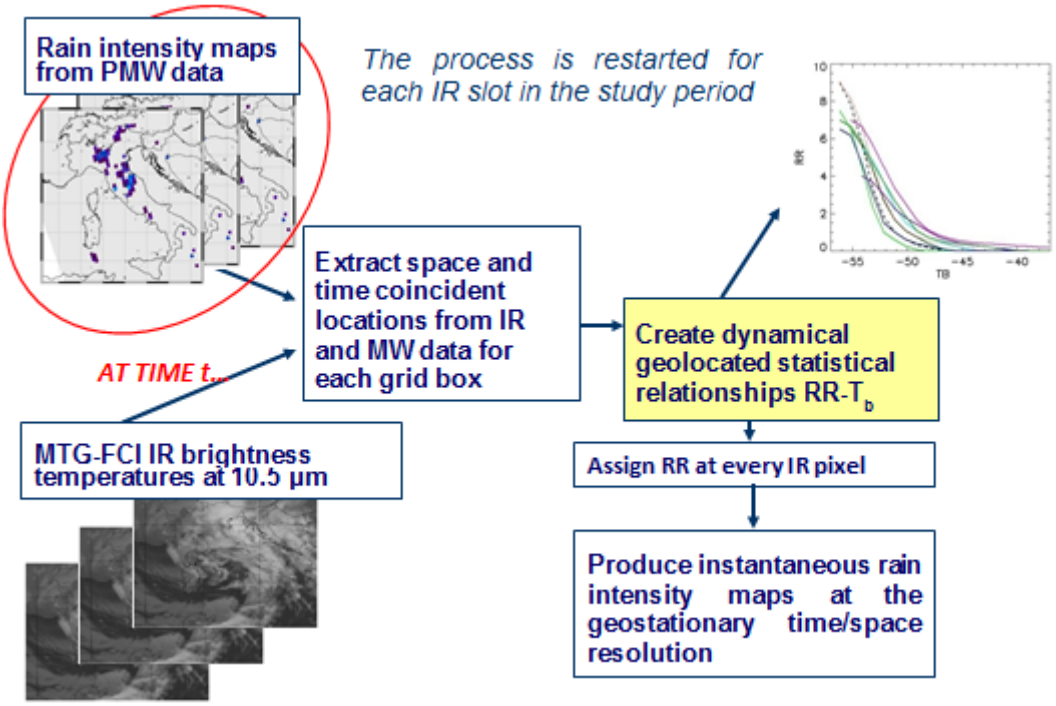

Figure 2: Main processing steps of the RU software package.

3.2 Additional developments

In the course of the H-SAF Development Phase, the RU algorithm was further developed in COMet at instances. Several implementations in the source code occurred, in particular:

• pre-screening of the IR data using the "Cloud Type" from NWC-SAF was added, that gives the possibility to clean the meteorological scene from cirrus, broken clouds and semitransparent clouds in general;
• parallel operational chain with a delay of 3 hours is implemented in order to include the polar MW inputs and to respect the expected timeliness.

During the H-SAF Continuous Development Phase-2 (CDOP-2) a quality flag was conceived and associated to the precipitation output of the RU software package with the aim of providing the end-users with a simple and immediate criterion for the evaluation of the P-IN-SEVIRI product. Two aspects were taken into account for the generation of the quality flag:

1) **Quality of the input PMW precipitation products**

The P-IN-SEVIRI product is based on the availability of PMW precipitation estimates used for the calibration of IR brightness. Thus its quality is linked to the quality of the PMW rainfall estimation input to the algorithms. The P-IN-SSMIS new release and P-IN-MHS quality flags are ingested in terms of percentage values by the RU algorithm and propagated through the code up to the assignment of a quality flag to each TB vs RR relationship (QF_{mw})

2) Monitoring the PMW precipitation flux timeliness

It is fundamental to monitor the flux of the PMW precipitation products used as inputs, by considering the time difference between the last PMW sensor overpass and the currently processing MSG slot ($diff_{time}$). This time tells the user how old the calibrations TBB vs RR are and thus how adequate they are to be used for the rain rate assignment. An index (QF_{time}) was modeled to represent the downgrade of the product quality:

$$QF_{time} = exp\left(\frac{-diff_{time}}{time_{limit}}\right) with time_{limit} = 5h$$

The total quality flag (QF_{total}), which summarizes the two aspects previously described, was generated as follows:

$$QF_{total} = \begin{cases} 0.5 * (QF_{time} + QF_{mw}) & if\ diff_{time} \leq 5h \\ 2/3 * QF_{time} + 1/3 * QF_{mw} & if\ diff_{time} \in]5, 10]h \\ QF_{time} & if\ diff_{time} > 10h \end{cases}$$

3.3 Processing steps overview

This section introduces the main processing steps, which are implemented in the P-IN-FCI processor. The package can be subdivided into four main parts, namely:

1) pre-processing: preparation and pre-processing of GEO data; preparation and pre-processing of PMW rain rate maps at the LEO space-time resolution.
2) co-location: co-located GEO and LEO observations are collected for the selected study area and accumulated from oldest to newest;
3) set-up of geo-located statistical relationships applying the probability matching technique;
4) assign rain rate to each GEO pixel: production of rain-rate maps at the GEO space-time resolution.

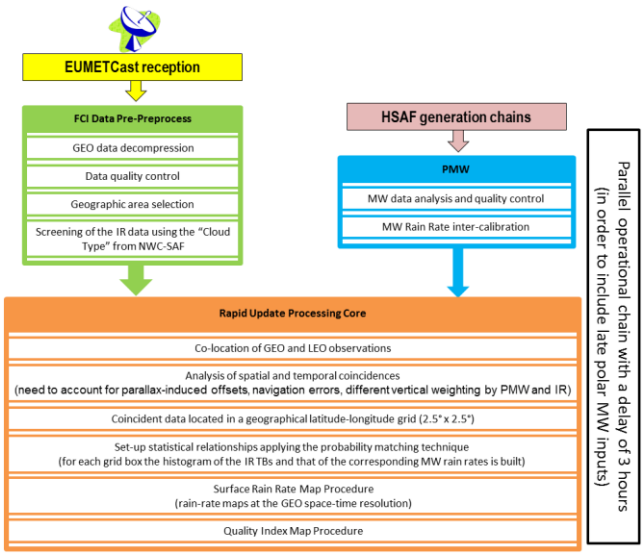

Figure 3. H40A/B block diagram.

The diagram in Fig. 3 describes the main functions of the general structure of the RU software package.

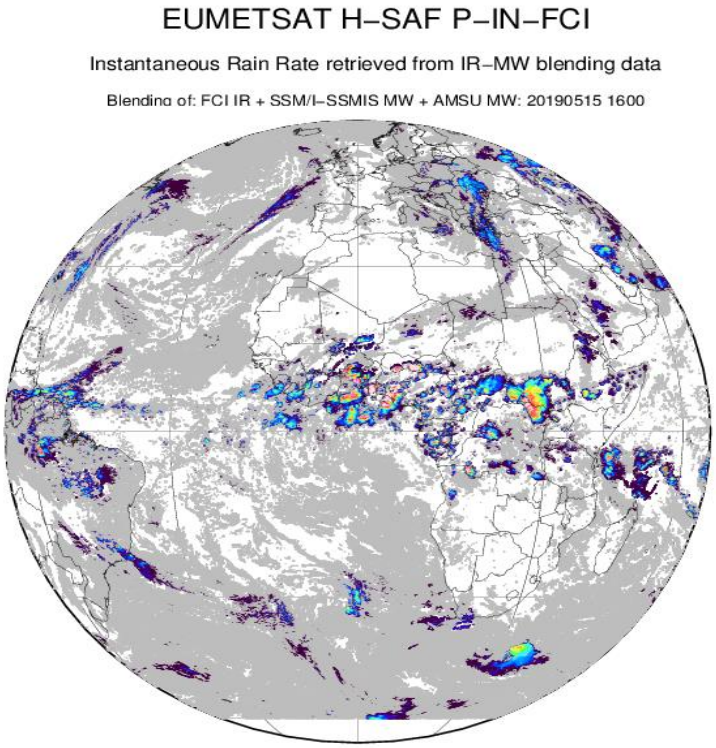

Figure 4: Example of the P-IN-FCI product

4 Validation activities of P-IN-FCI product

The validation methodology of the precipitation products in H-SAF area (European region) is composed by two components: one based on large statistics (multi-categorical and continuous), and one on selected case studies. Both components are considered complementary in assessing the accuracy of the implemented algorithms. Large statistics helps in identifying existence of pathological behavior; selected case studies are useful in identifying the roots of such behavior, when present.
During the CDOP-3 the availability of the satellite precipitation products over the full disk poses the problem of their validation outside Europe. In Africa there are few precipitation data derived by ground networks: the operational rain gauges stations are sparse and the radar networks are often not fully operational or not available at all. For all these reasons, the large statistic quality assessment in African region will be mainly focused on the comparison of H-SAF precipitation products with other satellite products as the Global Precipitation Mission (GPM) products derived by Dual-frequency (Ka-band and Ku-band) Precipitation Radar (DPR). Which GPM product would be used, if one-band

or dual-band together with the introduction of different analysis techniques, as triple collocation method, is still under discussion within the validation group.

5 References

Casella, D., Panegrossi, G., Sanò, P., Mugnai, A., Smith, E. A., Tripoli, G. J., Dietrich, S., Formenton, M., Leung, W.Y., and Mehta, A.: Transitioning from CRD to CDRD in bayesian retrieval of rainfall from satellite passive microwave measurements: Part 2. Overcoming database profile selection ambiguity by consideration of meteorological control on microphysics, IEEE T. Geosci. Remote, 51, 4650-4671, 2013.

Casella, D., Panegrossi, G., Sanò, P., Milani, L., Petracca, M., and Dietrich, S.: A novel algorithm for detection of precipitation in tropical regions using PMW radiometers, Atmos. Meas. Tech., 8, 1217–1232, doi:10.5194/amt-8-1217-2015, 2015.

Mugnai, A., Smith, E. A., and Tripoli, G. J.: Foundations for statistical physical precipitation retrieval from passive microwave satellite measurement. Part II : Emission-source and generalized weighting-function properties of a time-dependent cloud-radiation model, J. Appl. Meteorol, 32, 17-39, 1993.

Mugnai, A., Casella, D., Cattani, E., Dietrich, S., Laviola, S., Levizzani, V., Panegrossi, G., Petracca, M., Sanò, P., Di Paola, F., Biron, D., De Leonibus, L., Melfi, D., Rosci, P., Vocino, A., Zauli, F., Puca, S., Rinollo, A., Milani, L., Porcù, F., and Gattari, F.: Precipitation products from the hydrology SAF, Nat. Hazards Earth Syst. Sci, vol. 13, n. 8, pp. 1959-1981, doi:10.5194/nhess-13-1959-2013, 2013a.

Mugnai, A., Smith, E. A., Tripoli, G. J., Bizzarri, B., Casella, D., Dietrich, S., Di Paola, F., Panegrossi, G., and Sanò, P.: CDRD and PNPR satellite passive microwave precipitation retrieval algorithms: euroTRMM/EURAINSAT Origins and H-SAF operations, Nat. Hazards Earth Syst. Sci, vol. 13, pp. 887–912, doi:10.5194/nhess-13-887-2013, 2013b.

Panegrossi, G., Dietrich, S., Marzano, F. S., Mugnai, A., Smith, E. A., Xiang, X., Tripoli, G. J., Wang, P. K., and Poiares Baptista, J. V. P.: Use of cloud model microphysics for passive microwave-based precipitation retrieval: significance of consistency between model and measurement manifolds, *J. Atmos. Sci.*, vol. 55, pp. 1644-1673, 1998.

Panegrossi, G., Casella, D., Dietrich, S., Marra, A. C., Milani, L., Petracca, M., Sanò, P., and Mugnai, A.: CDRD and PNPR passive microwave precipitation retrieval algorithms: extension to the MSG full disk area, Proc. 2014 EUMETSAT Meteorological Satellite Conference, Geneva, https://www.eumetsat.int/website/home/News/ConferencesandEvents/DAT_2076129.html, 2014.

Panegrossi, G., Casella, D., Dietrich, S., Marra, A.C., Petracca, M., Sanò, P., Baldini, L., Roberto, N., Adirosi, E., Cremonini, R., Bechini, R., Vulpiani, G.: Use of the constellation of PMW radiometers in the GPM ERA for heavy precipitation event monitoring and analysis during fall 2014 in Italy, Int. Geosci. Remote Se., IGARSS 2015, pp. 5150-5153, doi: 10.1109/IGARSS.2015.7326993, 2015.

Panegrossi, G., Casella, D., Dietrich, S., Marra, A.C., Sanò, P., Mugnai, A., Baldini, L., Roberto, N., Adirosi, E., Cremonini, R., Bechini, R., Vulpiani, G., Petracca, M., and Porcù, F.: Use of the GPM Constellation for Monitoring Heavy Precipitation Events Over the Mediterranean Region, IEEE J. Sel. Top. Appl., vol. PP, n. 99, pp. 1-21, doi: 10.1109/JSTARS.2016.2520660, 2016.

Sanò, P., Casella, D., Mugnai, A., Schiavon, G., Smith, E. A., and Tripoli, G. J.: Transitioning from CRD to CDRD in bayesian retrieval of rainfall from satellite passive microwave measurements: Part 1. Algorithm description and testing, IEEE T. Geosci. Remote, 51, 4119-4143, doi: 10.1109/TGRS.2012.2227332, 2013.

Sanò, P., Panegrossi, G., Casella, D., Di Paola, F., Milani, L., Mugnai, A., Petracca, M., and Dietrich, S.: The Passive microwave Neural network Precipitation Retrieval (PNPR) algorithm for AMSU/MHS observations: description and application to European case studies, Atmos. Meas. Tech., vol. 8, pp. 837–857, doi:10.5194/amt-8-837-2015, 2015.

Sanò, P., Panegrossi, G., Casella, D., Marra, A., C., Di Paola, F., and Dietrich, S.: The new Passive microwave Neural network Precipitation Retrieval (PNPR) algorithm for the cross-track scanning ATMS radiometer: description and verification study over Europe and Africa using GPM and TRMM spaceborne radars, Atmos. Meas. Tech. Discuss., doi:10.5194/amt-2016-199, 2016.

Smith, E. A., Leung, H. W.-Y., Elsner, J. B., Mehta, A. V., Tripoli, G. J., Casella, D., Dietrich, S., Mugnai, A., Panegrossi, G., and Sanò, P.: Transitioning from CRD to CDRD in bayesian retrieval of rainfall from satellite passive microwave measurements: Part 3. Identification of optimal meteorological tags, Nat. Hazards Earth Syst. Sci, 13, 1185–1208, doi:10.5194/nhess-13-1185-2013, 2013.

Torricella F., V. Levizzani and F.J. Turk, 2007: “Application of a blended MW-IR rainfall algorithm to the Mediterranean”. In: Measuring precipitation from space – EURAINSAT and the future. V. Levizzani, P. Bauer, and F. J. Turk, Eds., Springer, 497-507.

Turk F.J., E.E. Ebert, B.-J. Sohn, H.-J. Oh, V. Levizzani, E.A. Smith and R.R. Ferraro, 2002: “Validation of an operational global precipitation analysis at short time scales”. Proc. 1st IPWG Workshop, Madrid, 23-27 Sept., 225-248.

Turk J.F., G. Rohaly, J. Hawkins, E.A. Smith, F.S. Marzano, A. Mugnai and V. Levizzani, 2000a: “Meteorological applications of precipitation estimation from combined SSM/I, TRMM and geostationary satellite data”. Microwave Radiometry and Remote Sensing of the Earth’s Surface and Atmosphere, P. Pampaloni and S. Paloscia Eds., VSP Int. Sci. Publisher, Utrecht (The Netherlands), 353-363.

Turk J.F., G. Rohaly, J. Hawkins, E.A. Smith, F.S. Marzano, A. Mugnai and V. Levizzani, 2000b: “Analysis and assimilation of rainfall from blended SSMI, TRMM and geostationary satellite data”. Proc. 10th AMS Conf. Sat. Meteor. and Ocean., 9, 66-69.

Turk J.F., B.-J. Sohn, H.-J. Oh, E.E. Ebert, V. Levizzani, and E.A. Smith, 2009: “Validating a rapidupdate satellite precipitation analysis across telescoping space and time scales”. Meteor. Atmos. Phys., 105, 99-108.

Calheiros R.V., Zawadzki I., 1987. “Reflectivity-Rain Rate Relationships for Radar Hydrology in Brazil”. Journal of climate and applied meterology vol.26

MTG-FCI L1 Product User Guide (FCIL1DUG), 2015.

Annex 1: Acronyms

AMSU	Advanced Microwave Sounding Unit (on NOAA and MetOp)
AMSU-A	Advanced Microwave Sounding Unit - A (on NOAA and MetOp)
AMSU-B	Advanced Microwave Sounding Unit - B (on NOAA up to 17)
ATDD	Algorithms Theoretical Definition Document
AU	Anadolu University (in Turkey)
BfG	Bundesanstalt für Gewässerkunde (in Germany)
CAF	Central Application Facility (of EUMETSAT)
CDOP	Continuous Development-Operations Phase
CESBIO	Centre d'Etudes Spatiales de la BIOsphere (of CNRS, in France)
CM-SAF	SAF on Climate Monitoring
COMet	Centro Operativo per la Meteorologia (in Italy)
CNR	Consiglio Nazionale delle Ricerche (of Italy)
CNRS	Centre Nationale de la Recherche Scientifique (of France)
DMSP	Defense Meteorological Satellite Program
DPC	Dipartimento Protezione Civile (of Italy)
EARS	EUMETSAT Advanced Retransmission Service
ECMWF	European Centre for Medium-range Weather Forecasts
EDC	EUMETSAT Data Centre, previously known as U-MARF
EUM	Short for EUMETSAT
EUMETCast	EUMETSAT's Broadcast System for Environmental Data
EUMETSAT	European Organisation for the Exploitation of Meteorological Satellites
FMI	Finnish Meteorological Institute
FTP	File Transfer Protocol
GEO	Geostationary Earth Orbit
HDF	Hierarchical Data Format
HRV	High Resolution Visible (one SEVIRI channel)
H-SAF	SAF on Support to Operational Hydrology and Water Management
IDL©	Interactive Data Language
IFOV	Instantaneous Field Of View
IMWM	Institute of Meteorology and Water Management (in Poland)
IPF	Institut für Photogrammetrie und Fernerkundung (of TU-Wien, in Austria), now Department of Geodesy and Geoinformation
IPWG	International Precipitation Working Group
IR	Infra Red
IRM	Institut Royal Météorologique (of Belgium) (alternative of RMI)
ISAC	Istituto di Scienze dell'Atmosfera e del Clima (of CNR, Italy)
ITU	İstanbul Technical University (in Turkey)
LATMOS	Laboratoire Atmosphères, Milieux, Observations Spatiales (of CNRS, in France)
LEO	Low Earth Orbit
LSA-SAF	SAF on Land Surface Analysis
Météo France	National Meteorological Service of France
METU	Middle East Technical University (in Turkey)
MHS	Microwave Humidity Sounder (on NOAA 18 and 19, and on MetOp)
MSG	Meteosat Second Generation (Meteosat 8, 9, 10, 11)
MVIRI	Meteosat Visible and Infra Red Imager (on Meteosat up to 7)
MW	Micro Wave
NESDIS	National Environmental Satellite, Data and Information Services
NMA	National Meteorological Administration (of Romania)
NOAA	National Oceanic and Atmospheric Administration (Agency and satellite)
NRT	Near real-time
NWC-SAF	SAF in support to Nowcasting & Very Short Range Forecasting
NWP	Numerical Weather Prediction
NWP-SAF	SAF on Numerical Weather Prediction
O3M-SAF	SAF on Ozone and Atmospheric Chemistry Monitoring
OMSZ	Hungarian Meteorological Service
ORR	Operations Readiness Review
OSI-SAF	SAF on Ocean and Sea Ice

PDF	Probability Density Function
PEHRPP	Pilot Evaluation of High Resolution Precipitation Products
Pixel	Picture element
PMW	Passive Micro-Wave
PP	Project Plan
PPF	Product Processing Facility
PR	Precipitation Radar (on TRMM)
PUM	Product User Manual
PVR	Product Validation Report
RMI	Royal Meteorological Institute (of Belgium) (alternative of IRM)
RR	Rain Rate
RU	Rapid Update
SAF	Satellite Application Facility
SEVIRI	Spinning Enhanced Visible and Infra-Red Imager (on Meteosat from 8 onwards)
SHMÚ	Slovak Hydro-Meteorological Institute
SSM/I	Special Sensor Microwave / Imager (on DMSP up to F-15)
SSMIS	Special Sensor Microwave Imager/Sounder (on DMSP starting with S-16)
SYKE	Suomen ympäristökeskus (Finnish Environment Institute)
T_{BB}	Equivalent Blackbody Temperature (used for IR)
TKK	Teknillinen korkeakoulu (Helsinki University of Technology)
TMI	TRMM Microwave Imager (on TRMM)
TRMM	Tropical Rainfall Measuring Mission
TSMS	Turkish State Meteorological Service
TU-Wien	Technische Universität Wien (in Austria)
U-MARF	Unified Meteorological Archive and Retrieval Facility
UniFe	University of Ferrara (in Italy)
URD	User Requirements Document
UTC	Universal Coordinated Time
VIS	Visible
ZAMG	Zentralanstalt für Meteorologie und Geodynamik (of Austria)